Transpiration Cooling of a Turbulent Boundary Layer in an Axisymmetric Nozzle

JOSEPH LIBRIZZI* AND ROBERT J CRESCI†
Polytechnic Institute of Brooklyn, Freeport, N Y

This report presents the results of an experimental investigation of the downstream influence of mass transfer on the heat transfer to an axisymmetric nozzle in turbulent flow Helium and nitrogen are used as coolants and are injected through a porous region upstream of the nozzle throat at various rates The high-temperature environment is obtained by burning methane and oxygen in a chamber well upstream of the model Stagnation temperatures of between 1600° and 2600°R were achieved; the gas mixture obtained corresponds to an average specific heat ratio of 1 29 The experimental heat transfer is presented, in terms of an appropriate similarity parameter, as a function of coolant injection rate for various stations along the nozzle surface Also presented is an approximate analysis for the prediction of the variation of heat transfer with coolant injection rate to the impermeable surface The results of the experiments show a decrease in heat transfer with an increase in mass injection, helium being more effective for the same mass flow rate than nitrogen This decrease in heat transfer becomes less prominent as the distance downstream of the porous region increases

Nomenclature

B = $Re^{0.8}/\bar{N}_1\bar{N}_R^{0.8}$, mass-transfer parameter of Ref 10
c_f = skin-friction coefficient
c_p = specific heat at constant pressure
h = enthalpy
$\bar{h}$ = h/h_e
k = thermal conductivity
m = mass flow of injected gas per unit time
M = molecular weight
$\bar{M}$ = molecular weight of gaseous mixture
n = coordinate normal to surface
N_1 = mass-transfer similarity parameter for laminar flow [Eq (4)]
$\bar{N}_1$ = mass-transfer similarity parameter for turbulent flow [Eq (2)]
N_2 = heat-transfer similarity parameter for laminar flow [Eq (3)]
$\bar{N}_2$ = heat-transfer similarity parameter for turbulent flow [Eq (1)]
Nu = $(q_w r^* c_{p_e}/k)/(h - h_w)$, Nusselt number
$\bar{N}_R$ = $(\rho_s h_s^{1/2} r^*/\mu)\varphi_e^{1/2}$, Reynolds number
p = pressure
q = local heat-transfer rate
r = radius of nozzle measured from the centerline
r^* = radius of nozzle throat
$\bar{r}$ = r/r^*, ratio of nozzle radius to throat radius
Re_x = $\rho_e u x/\mu_e$, local Reynolds number
s = space coordinate along the surface (measured from the initiation of the injection region)
$\bar{s}$ = s/r^*, nondimensionalized space coordinate along surface
t = wall thickness
T = temperature
u = velocity parallel to the surface
$\bar{u}$ = $u/h_{s_e}^{1/2}$, nondimensionalized velocity
v = velocity normal to the surface
X = mole fraction
γ = ratio of specific heats
$\bar{\gamma}$ = ratio of specific heats of gaseous mixture
δ = boundary-layer thickness
δ^* = displacement thickness
η = space coordinate normal to surface
θ = momentum thickness
μ = viscosity coefficient
ρ = mass density
$\bar{\rho}$ = ρ/ρ_s, nondimensionalized density
σ = $\mu c_p/k$, Prandtl number
φ = $p_{s_e}/\rho h$, real gas parameter

Subscripts

aw = conditions evaluated at the wall temperature for the case of zero heat transfer
c = coolant gas characteristics prior to injection
e = local conditions external to the boundary layer
i = conditions evaluated at the termination of the injection region
0 = conditions corresponding to zero injection
s_e = conditions external to the boundary layer at the stagnation region
w = conditions evaluated at the wall
w_i = conditions evaluated at the water-cooled surface of the nozzle wall

Received August 2, 1963; revision received January 7, 1964 This research was carried out at the Polytechnic Institute of Brooklyn, Aerodynamics Laboratory, under Contract No AF 33(616)-7661 This contract is administered by the Aeronautical Research Laboratories, Office of Aerospace Research, U S Air Force The authors are pleased to acknowledge the assistance of the hypersonic and computing staffs of Polytechnic Institute of Brooklyn Aerodynamics Laboratory in carrying out this research, and of Paul A Libby for initiating the investigation and for his helpful suggestions in the research discussed herein

* Formerly Research Assistant; now Associate Scientist, Research and Advanced Development Division, Avco Manufacturing Corporation, Wilmington, Mass
† Research Associate Professor of Aerospace Engineering

Introduction

THE problem of effectively cooling a nozzle operating under conditions of high local heat flux has existed for some time Recent advances in rocket-motor development as well as the development of high-enthalpy wind-tunnel facilities have intensified this problem to the point where conventional cooling methods may no longer be feasible Convective or regenerative cooling has been used successfully in the past; however, the maximum heat rate capable of being dissipated by this method is on the order of 5000 Btu/ft²-sec This rate can easily be exceeded in the throat of a wind-tunnel nozzle, e g , operating from an arc heater source

Eckert and Livingood[1] have compared the relative effectiveness of convection, film, and transpiration cooling and have found that, on the basis of equal coolant flow rates, transpiration cooling is the most effective system Transpiration cooling, however, when applied to an entire nozzle, i e , a completely porous nozzle, is not feasible since materials with uniform porosity and suitable strength characteristics

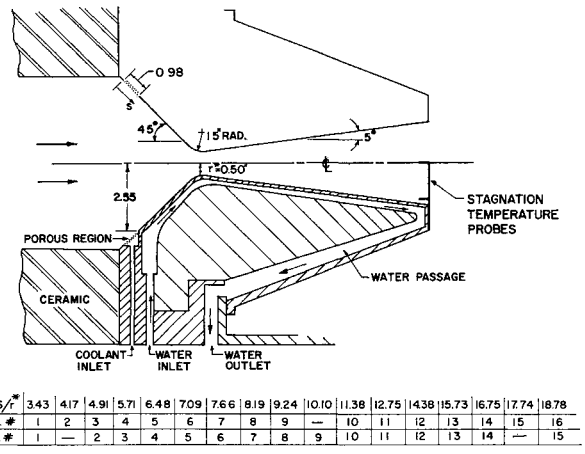

s s/r*	3.43	4.17	4.91	5.71	6.48	7.09	7.66	8.19	9.24	10.10	11.38	12.75	14.38	15.73	16.75	17.74	18.78
T.C. #	1	2	3	4	5	6	7	8	9	—	10	11	12	13	14	15	16
P.T. #	1	—	2	3	4	5	6	7	8	9	10	11	12	13	14	—	15

Fig 1 Model detail and instrumentation

are not presently available As a result, for a practical application of this method, one usually considers small regions of porous material adjacent to impermeable surfaces The coolant fluid is then injected in a sufficient quantity to cool the permeable surface completely and the impermeable surface to a lesser extent

The problem investigated in this paper is that of the downstream influence of mass injection through a porous region of an axisymmetric nozzle in turbulent flow A schematic diagram of the mass-transfer system and coordinate system considered is shown in Fig 1 The coolant gas is injected into the boundary layer of the nozzle in an essentially stagnant region; the local area ratio (A/A^*) is designed to be sufficiently large to limit the maximum external flow velocity to below 25 fps This minimizes the extent of localized separation in this region because of the sharp internal corner In addition, the porous region is not immediately adjacent to the corner and, as a result, is not influenced by any localized separation that may occur Another consideration in the choice of the injection region location was to attempt to cool the entire subsonic portion of the nozzle It is realized that the portion of the nozzle which experiences the highest convective heat flux is the throat region However, for high stagnation enthalpy applications, the heat flux to the entire subsonic region may be critical The influence of the injected coolant on the heat transfer to the entire impermeable region, therefore, is of prime concern

The turbulent boundary layer on a porous surface with both homogeneous and heterogeneous mass transfer has been treated fairly extensively in the literature Rubesin and Pappas[2, 3] developed theoretical analyses of the effect of transpiration cooling on the turbulent boundary-layer characteristics; the coolants considered were air, helium, and hydrogen These analyses were correlated[4] in terms of a similarity parameter that practically eliminates the effect of external Mach number and Reynolds number Black and Sarnecki[5] conducted a detailed investigation of the velocity profiles occurring in a turbulent layer with homogeneous mass transfer In obtaining an analytical expression for the modified sublayer and "law of the wall," a large number of experimentally obtained profiles were used Additional experimental data in terms of both velocity and temperature profiles are available in Refs 6–9

Investigation of the region downstream of the transpiration-cooled surface, however, has received little attention Reference 10 presents experimentally obtained boundary-layer profiles downstream of a transpiration-cooled region in a low-speed turbulent flow An integral method is developed therein which is based on the experimental profiles; the predicted adiabatic wall temperature was found to agree reasonably well with the experimental data

More closely related to the present problem is Ref 11, which deals with a transpiration-cooled two-dimensional nozzle The test pressures were relatively low, however, resulting in a laminar boundary layer Two test nozzles were used, each having the porous region at a different position with respect to the nozzle throat Helium and air were used as coolants The results show an appreciable decrease in the equilibrium surface temperature with respect to the zero injection case, with the decrease due to helium persisting for a greater distance downstream of the injection area than that with homogeneous injection

In the present paper there are presented the results of an experimental investigation of turbulent heat transfer to the impermeable surface of a transpiration-cooled nozzle The method for obtaining the high-energy gas flow and the test procedure are described first The data-reduction procedure is explained, and the similarity parameters used to present the downstream heat-transfer rates and coolant mass flow rates are discussed Finally, an approximate downstream analysis is presented and compared to the present data and also to data obtained for a turbulent flow over a flat plate in low-speed flow [10]

Model Design and Test Procedure

Details of the model construction and instrumentation are shown in Fig 1 The test nozzle is made of stainless steel with a wall thickness 0 10 in The porous region is constructed of sintered stainless steel and has a mean pore size of approximately 50 μ Other pertinent physical dimensions are given in Fig 1 The coolant is supplied to the coolant chamber, which is essentially a stagnation region, by two inlet lines; the rate at which it is injected into the main flow is regulated by the pressure drop across the porous plate The inside surface of the nozzle skin is cooled by the flow of water through the passage (cf Fig 1) which is designed such that the maximum velocity of the water and, as a result, the maximum cooling rate are achieved in the region of the nozzle throat

The pressure taps and thermocouples are diametrically opposed on the surface of the nozzle and are located as indicated in Fig 1 The coordinate used in the table in Fig 1 is measured along the surface of the nozzle and originates at the initiation of the porous region, as shown The pressure is recorded continuously during a test by means of transducers connected to strip chart recorders In addition to the thermocouples that measure the heated surface temperature, there are several thermocouples located on the inner (water-cooled) surface These thermocouples are used to determine the temperature distribution along the inner surface As indicated in the following section, the heat flux to the wall is obtained by using the difference between these two temperatures

The combustion chamber configuration is used to obtain a relatively high-temperature fluid in order to study the feasilbility of transpiration cooling in a nozzle A typical test procedure is as follows The main air supply is turned on, and subsequently the spark, cooling water, and gaseous coolant flow are initiated in sequence The methane is then turned on and proceeds to burn in a rich mixture A leaner mixture is obtained by adding pure oxygen and simultaneously increasing the tunnel pressure until the desired test conditions are achieved The high-energy combustion products pass through a ceramic nozzle in which the flow remains completely subsonic; this serves as a radiation shield for the test nozzle and also tends to eliminate any nonuniformities in the flow When a steady temperature and pressure are obtained in the test chamber, the model thermocouples are monitored, and when no further variations with time are apparent, the test is terminated The heat-transfer results are obtained from a steady-state analysis of the heated and cooled surface temperatures

Since the test gas is not pure air but is composed of the combustion products of air and methane, it is necessary to determine its composition; this is then used to determine the various thermodynamic and transport properties that are required in the data reduction and analysis Knowledge of the initial mass fractions of the various constituents is required, therefore, in the determination of the combustion products The mass flows of methane and oxygen are obtained by means of flowmeters inserted into the supply lines of the two gases The main air mass flow is too large to be measured with an available flowmeter and, as a result, is obtained by calculating the total mass flow passing through the choked nozzle throat and subtracting the known mass flows of the methane, oxygen, and coolant fluids The boundary-layer displacement thickness at the nozzle throat was estimated in order to determine an effective throat area for each test; the maximum reduction in area amounted to roughly 5% of the geometric throat area Since the total mass flow through the nozzle can be determined only if the chamber conditions (p and T) and gas composition (specifically, $\bar{\gamma}$ and $\bar{M}$) are known, an iteration procedure is necessary Using an initial ratio of specific heats equal to 1 3 and molecular weight of 28 0, the total mass flow is determined, and the resulting chamber composition is also known These results are used to determine a second approximation to the total mass in the nozzle; in all of the tests, the change in the final composition due to the second approximation was less than 1% for any component

The coolant flow rate is obtained by two methods; one consists of inserting a flowmeter in the coolant supply line and measuring the mass flow directly The other method involves measuring the pressure drop across the porous plate and comparing this with a calibration curve of mass flow vs pressure drop which was obtained under ambient conditions prior to the test program In all tests, the values obtained from both of these measurements agreed within 10%

The stagnation temperature of the flow is measured at the exit of the nozzle There are two temperature probes, one at the centerline of the nozzle and one in the proximity of the nozzle wall but well outside the boundary layer This is done to eliminate any reading error caused by the flame radiation from the combustion chamber In all tests, the two probes read within 50°F of each other; there was no observable correlation between the location and the high reading probe

The tests reported herein were performed at a stagnation pressure of approximately 200 psia and stagnation temperatures varying between 1600° and 2600°R; the test fluid was found to correspond, as will be discussed in more detail below, to a gas with an average ratio of specific heats equal to 1 29 and with a molecular weight of 27 6

Both coolant gases were injected at a temperature of approximately 520°R Since the coolant flow rates were relatively large, the porous surface was assumed to remain at the coolant temperature throughout the test The steady-state impermeable surface temperature varied along the surface, reaching a maximum value at the throat The average ratio of wall to stagnation enthalpy, $\bar{h}_w$, varied between 0 25 for $\bar{s} \sim 2\ 0$ and 0 37 for $\bar{s} \sim 8\ 0$ In the supersonic portion of the nozzle, $\bar{h}_w$ decreased to roughly 0 3 at the nozzle exit

Data Analysis and Presentation

The results of the experiments are presented in terms of the similarity parameters for a compressible turbulent boundary layer with mass transfer; these are as follows:

$$\bar{N}_2 = Nu/\bar{N}_R{}^{4/5} \tag{1}$$

$$\bar{N}_1 = m/r^*\mu\ \bar{N}_R{}^{4/5} \tag{2}$$

The applicability of the first similarity parameter ($\bar{N}_2$), which is indicative of the heat transfer to the impermeable surface, is demonstrated in Refs 12 and 13 The development of this parameter is dependent upon the Prandtl skin-friction law ($c_f/2 = 0\ 013/Re_\theta{}^{1/4}$)

The second of these parameters ($\bar{N}_1$) is proportional to the mass flow of the coolant; this parameter is suggested by an examination of the corresponding similarity parameters for laminar flow These were developed in Ref 14 and are given below:

$$N_2 = Nu/\bar{N}_R{}^{1/2} \tag{3}$$

$$N_1 = m/r^*\mu\ \bar{N}_R{}^{1/2} \tag{4}$$

The parameter ($\bar{N}_1$) for turbulent flow can thus be inferred from Eq (4) if the laminar variation of N_1 with Reynolds number is modified in the same manner as in the heat-transfer parameter A further justification of the use of this parameter can be seen by consideration of the results of Ref 3 The analysis performed therein determines the effect of mass transfer on the boundary-layer characteristics In particular, the ratio of the skin-friction coefficient with injection to that without injection is given as a function of a mass flow parameter:

$$c_f/c_{f_0} = f(2F/c_{f_0}) \tag{5}$$

where $F = \rho_w v_w/\rho\ u$

If the Prandtl skin-friction law is used to relate c_{f_0} and the local Reynolds number based on momentum thickness, manipulation of the quantity $2F/c_{f_0}$ yields

$$2F/c_{f_0} = \bar{N}_1 f(M, Re) \tag{6}$$

Therefore, the skin-friction ratio is found to be a function of $\bar{N}_1$ and the external flow properties The heat-transfer rate can also be shown to depend on $\bar{N}_1$ in a similar manner

In order to calculate the various quantities required to form these similarity parameters from the experimental data, the composition of the gas mixture must be obtained The method used is described by Penner[15]; the numerical values of the required equilibrium constants are also obtained therefrom

The stagnation temperature and pressure, which are two of the quantities needed to determine the composition, are obtained by direct measurement The number of moles of reactants are determined by dividing the mass flow rates of the components by their corresponding molecular weights The resulting mixture composition therefore enables one to calculate such quantities as the specific heat ratio, molecular weight, and total enthalpy The average values of molecular weight ($\bar{M}$) and specific heat ratio ($\bar{\gamma}$) for all tests were found to be 27 6 and 1 29, respectively The maximum deviation from the average, in any particular run, is 3 4% for the specific heat ratio and 5 8% for the molecular weight Consequently, these average values are used in all of the theoretical analyses, whereas in the data reduction the individual composition for each run was used

Since, in general, the external flow composition is not constant in a reacting mixture with varying static temperature and pressure, the limiting cases of frozen flow and equilibrium are considered Several calculations were carried out in which the equilibrium composition, at different surface locations along the nozzle, was obtained for a given run The results of this calculation indicated a negligible variation in the mixture composition with distance along the nozzle, and, as a result, the test fluid was assumed to be of constant chemical composition

The thermodynamic and transport properties of interest can be determined once the chemical composition of the external flow is known Approximate expressions for the Prandtl number and viscosity coefficient for a multicomponent mixture can be obtained from Ref 16; these are

$$\sigma = 4\bar{\gamma}/(9\bar{\gamma} - 5) \tag{7}$$

$$\mu = 46\,6 \times 10^{-10}(\bar{M})^{0\,5}(T)^{0\,6} \text{ lb/in -sec} \quad (8)$$

The computation of the wall enthalpy (necessary for the Nusselt number evaluation) is approximate in that the wall concentration of the coolant gas is not known As a result, the wall enthalpy used is obtained from the composition of the gaseous mixture at the edge of the boundary layer evaluated at the wall temperature

In computing $\bar{N}_2$, the local heat flux to the wall is required; this can be obtained by applying the basic method of Ref 17 to the inverse problem The problem to be solved in connection with the present data involves the solution of the steady-state, two-dimensional, heat-conduction equation for an axisymmetric shell It is required to determine the surface heat-transfer rate for a known distribution of temperature on the exposed and cooled surfaces The temperature is therefore expanded in terms of a wall thickness parameter as follows:

$$T(n,s) = T_0(n,s) + \epsilon T_1(n,s) + \epsilon^2 T_2(n,s) +$$

where $\epsilon = t/2r^*$ and t = wall thickness The terms in the heat-conduction equation involving the shell geometry are

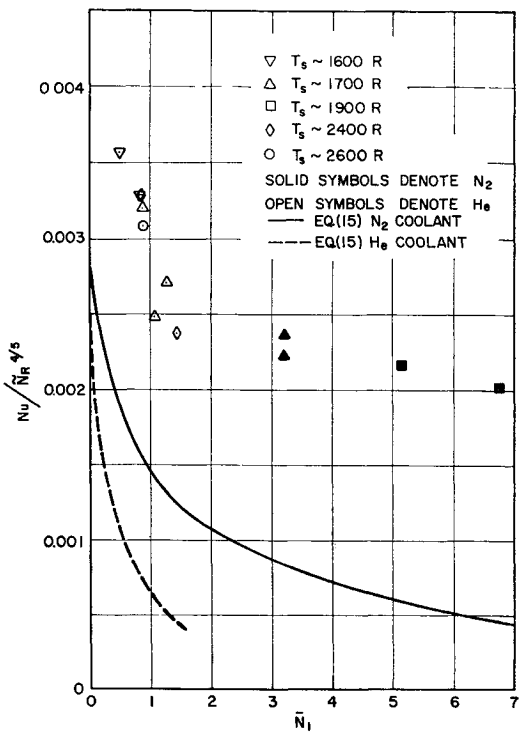

Fig 2a Variation of heat transfer with mass transfer, $\bar{s}$ = 4 17

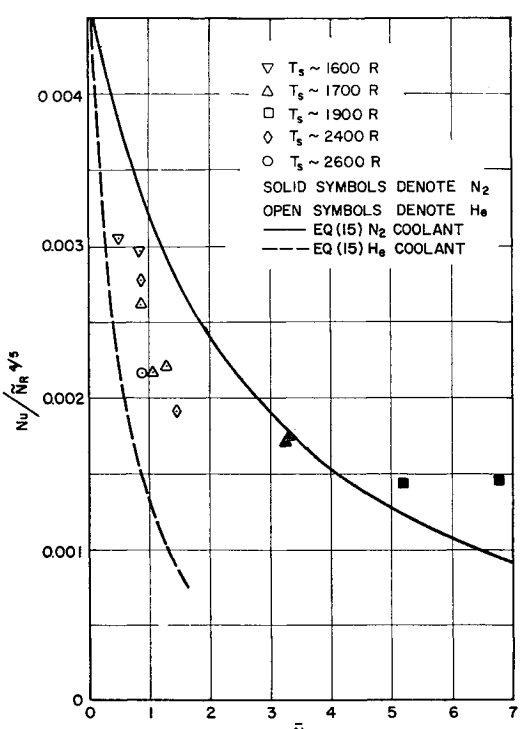

Fig 2b Variation of heat transfer with mass transfer, $\bar{s}$ = 5 71

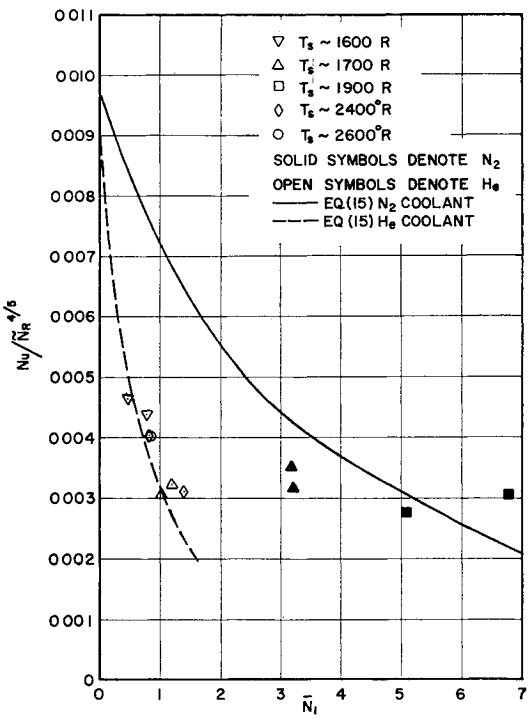

Fig 2c Variation of heat transfer with mass transfer, $\bar{s}$ = 7 09

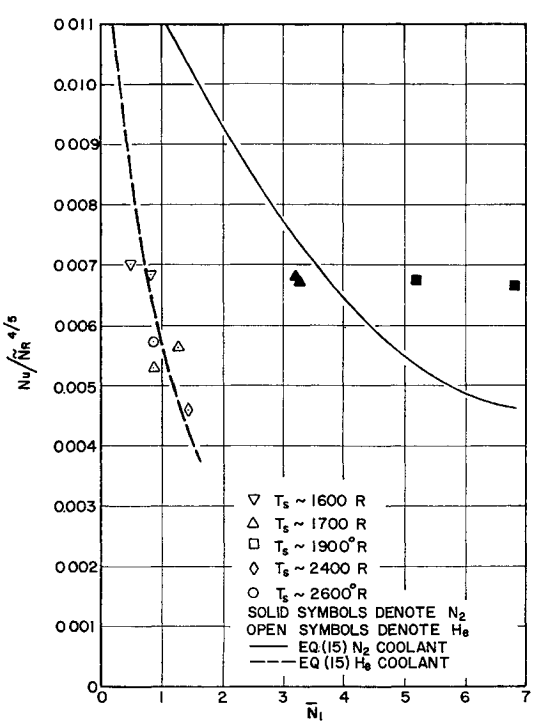

Fig 2d Variation of heat transfer with mass transfer, $\bar{s}$ = 9 24

expanded in a similar manner Substituting the temperature expression just given into the general heat-conduction equation and collecting terms with coefficients of the same exponent of ϵ results in a system of quasi-one-dimensional heat-conduction equations which can be solved using standard techniques The surface heat-transfer rate is then determined in terms of the exposed surface temperature and the temperature of the cooled surface as follows:

$$q_w = [T_w - T_{wi}]\left[1 - \frac{\epsilon g_0}{2}\right] + \epsilon^2 f\left[\frac{\partial T_w}{\partial s}, \frac{\partial^2 T_w}{\partial s^2}, \frac{\partial T_{wi}}{\partial s}, \text{etc}\right]$$

where g_0 is a function of the local radius of curvature of the surface, the distance from the centerline, and the local surface inclination It is evident that the surface conduction effects are of higher order (for relatively large values of heat flux) and therefore can be neglected in the computation of the local heat-transfer rate The correction term ($\epsilon g_0/2$) due to the nozzle geometry is retained in the computation and has a maximum value on the order of 0 15 in the throat region, where the local curvature is high

The experimental data are therefore presented in Figs 2a–2h, where the heat-transfer parameter ($\bar{N}_2$) is shown as a function

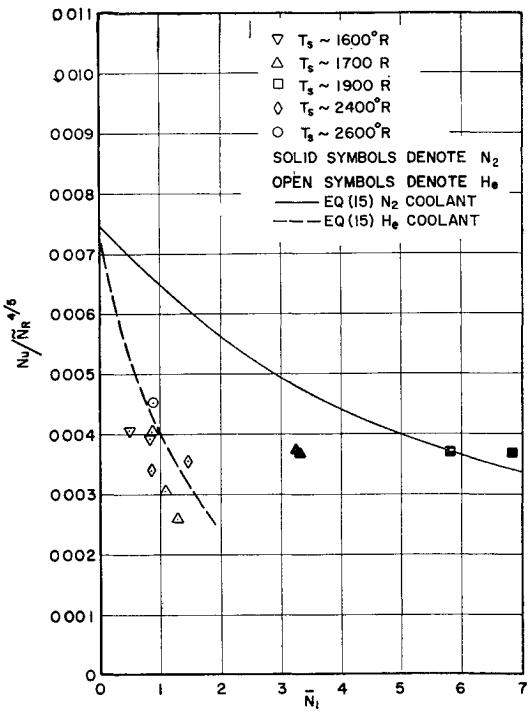

Fig 2e Variation of heat transfer with mass transfer, $\bar{s}$ = 12 75

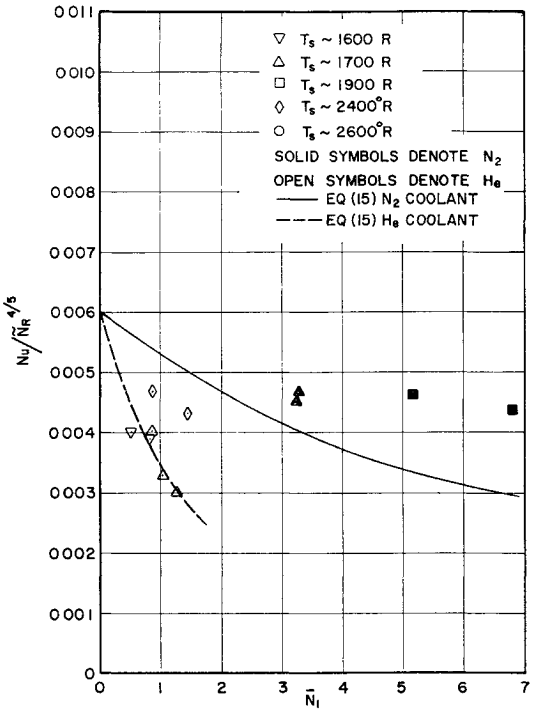

Fig 2f Variation of heat transfer with mass transfer, $\bar{s}$ = 14 38

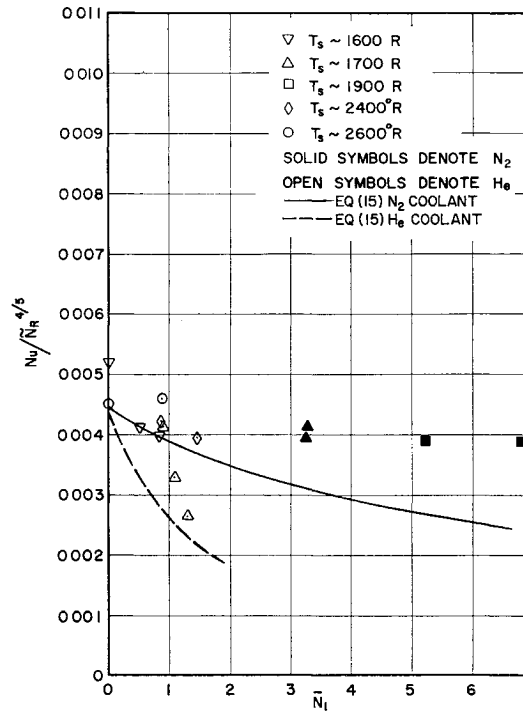

Fig 2g Variation of heat transfer with mass transfer, $\bar{s}$ = 16 75

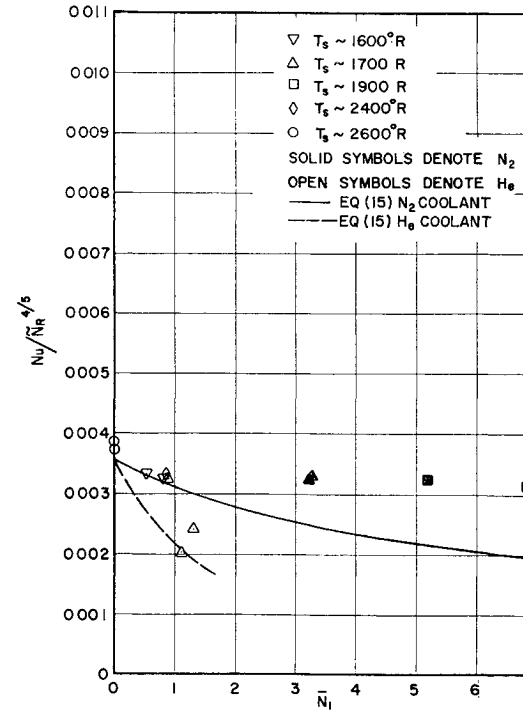

Fig 2h Variation of heat transfer with mass transfer, $\bar{s}$ = 18 78

tion of the mass transfer ($\bar{N}_1$) for typical‡ thermocouple locations The data for both the helium and nitrogen coolants are shown with the corresponding stagnation temperature for each run

All helium injection data presented in the figures correspond to a Reynolds number ($\bar{N}_R$) range between 0 3 × 10^6 and 1 0 × 10^6; the Reynolds number range for the nitrogen data is 0 6 × 10^6 to 0 8 × 10^6 Data obtained at lower Reynolds numbers than 0 3 × 10^6 for all injection rates, correspond to a transitional boundary layer and therefore could not be presented in terms of the similarity parameters used herein In addition to the Reynolds number limitation, it was observed that all the data obtained at surface locations

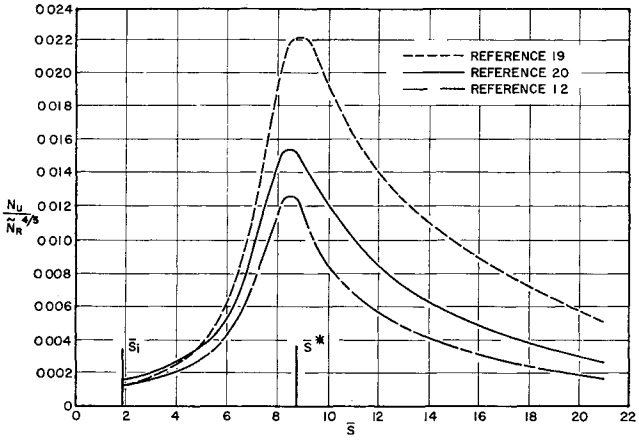

Fig 3 Zero injection turbulent heat-transfer theories

of $\bar{s} < 16\,0$ for values of the mass-transfer parameter $\bar{N}_1 < 0\,5$ also exhibited a variation with Reynolds number which did not coincide with either the predicted laminar or turbulent variation As a result, data corresponding to a value of the mass-transfer parameter ($\bar{N}_1$) lower than 0 5 are also omitted This interdependence of Reynolds number and mass-transfer rate on the location of the transition point has been observed previously, e g , Ref 18 Therein it was shown experimentally that, for a given Reynolds number, the transition point moved downstream as the mass-transfer rate decreased This was also evident in the present tests, wherein the data at large values of $\bar{s}(\bar{s} > 16\,0)$ were able to be correlated according to the turbulent heat-transfer parameter even for zero mass transfer (cf Figs 2g and 2h) For these surface locations the zero injection data at two different Reynolds numbers agreed reasonably well in terms of the similarity parameter $\bar{N}_2$, implying that fully developed turbulent flow was achieved at this station For $\bar{N}_1 = 0$ at smaller values of $\bar{s}$, however, there was no such agreement between the data corresponding to different test Reynolds numbers

Theoretical Analyses and Comparison with Experiment

In order to evaluate the efficacy of the mass transfer system, the zero injection heat-transfer distribution is required for comparison It is of interest, therefore, to examine several turbulent heat-transfer theories, since zero injection heat rates were not obtained experimentally Although there are available many theoretical analyses that may be applicable (cf Ref 13), only three methods will be considered herein These are the analysis of Bartz,[19] the integral method of Cresci, MacKenzie, and Libby,[12] and the flat-plate reference enthalpy method of Eckert[20] (cf also Ref 12) Figure 3 presents a comparison of these three methods evaluated for the present nozzle geometry The stagnation conditions, molecular weight, and specific heat ratio used in the computation of these curves constitute an average of the values obtained from the present tests; the stagnation temperature and pressure used are 2000°R and 200 psi, respectively It is seen that there is a relatively wide range in the heat-transfer rates predicted by the various theories, the highest being given by the analysis of Ref 19 and the lowest by the results of Ref 12 Since the present experiments provided insufficient fully turbulent zero injection data to substantiate any of these analyses, the experimental results of others are used to give an indication as to which of these theories is most applicable

References 21 and 22 present a comparison between experimental data and the theoretical predictions of Ref 19 for nozzles with different geometry The results of Ref 22 correspond to nozzles of three different contraction-area ratios; they are 8 to 1, 4 to 1, and 1 64 to 1 For all nozzles tested, the values of the experimental heat flux in the chamber section and contraction region of the nozzle are seen to be higher than the prediction of Ref 19 The peak values of the heat flux, however, are overestimated for the nozzle with an 8 to 1 contraction-area ratio and underestimated for the 1 64 contraction-area ratio nozzle The results of Ref 21, in which a nozzle of contraction-area ratio of 8 to 1 was used, are in accordance with this trend The contraction-area ratio for the nozzle tested herein is 50 to 1, which seems to indicate that the prediction of Ref 19 will overestimate the present data to some extent, except in the region of large area ratio (or low external Mach number) As a result of these considerations, the "flat-plate reference enthalpy" (FPRE) method of Ref 20 was chosen to represent the zero injection, heat-transfer distribution for the present test data This method predicts a lower rate of heat transfer than that of Ref 19 everywhere except in the low Mach number region of the nozzle; for this region, however, the data of Ref 22 are considerably higher than the predictions of any of the analyses considered herein It is unfortunate that the tests reported herein could not be run at sufficiently high Reynolds numbers to provide more fully turbulent data without mass transfer to substantiate this choice The use of the FPRE method is not completely arbitrary, however, since it has previously been shown to give excellent agreement with experiments for a wide variety of external flow fields (cf Refs 12, 13, 23, and 24) In addition, the few data points obtained in the present tests which do correspond to fully developed turbulent flow with no mass addition ($\bar{s} > 16\,0$) agree quite well with the FPRE method (cf Figs 2g and 2h) It would be of interest to apply this method to the experimental results of Refs 21 and 22 as well; however, there was not sufficient test information available in these references to perform this comparison

The theoretical analysis of boundary-layer characteristics on an impermeable surface downstream of a region with mass transfer invariably leads to involved numerical computations even for laminar flow (cf Refs 25–27) For a turbulent boundary layer, the required assumptions concerning velocity and temperature profiles, form factor, skin-friction coefficient, etc , do not warrant an involved analysis As a result, an attempt to predict the downstream effect of mass transfer was made using a relatively simple flow model § In essence, the low-enthalpy coolant is assumed to mix completely with the high-enthalpy fluid in the zero injection boundary layer, resulting in an average enthalpy lower than that of the external flow The stagnation enthalpy in the boundary layer with no mass transfer is assumed to be equal to the external stagnation enthalpy of the flow The re-

‡ The complete set of data for all the thermocouple locations indicated in Fig 1 is presented in Ref 29

§ This model of complete mixing of the two layers was suggested to the authors by Paul A Libby

sulting mass-averaged stagnation temperature is assumed uniform across the boundary-layer thickness and, therefore, represents the effective adiabatic wall temperature of the impermeable surface with upstream mass transfer

Consider quantitatively this model; the energy balance between the coolant and external fluid results in the following equation:

$$m_c[h_{aw} - h_c] = m_0[h - h_{aw}] \quad (9)$$

where h_{aw} is the enthalpy of coolant at the effective adiabatic wall temperature, h_{aw} is the enthalpy of external fluid at the effective adiabatic wall temperature, m is the coolant mass flow, and m_0 is the mass flow existing in the boundary layer with zero mass transfer The effective adiabatic wall temperature can therefore be obtained from Eq (9) for any coolant gas if the external flow conditions, coolant mass, and coolant temperature are known

The mass flow in the boundary layer of an axisymmetric nozzle without coolant injection is given by

$$m_0 = 2\pi r\rho\, u\,(\delta - \delta^*) = 2\pi r^* \mu_e \bar{\mu} r N_{R\theta}[(\delta/\theta) - (\delta^*/\theta)] \quad (10)$$

$N_{R\theta}$ can be obtained from the momentum equation for an axisymmetric boundary layer, which can be written in the form (cf Ref 12)

$$dN_{R\theta}/d\bar{s} = (\bar{N}_R/\varphi^{1/2})(\bar{\rho}\bar{u}/\bar{\mu})(c_f/2) - N_{R\theta}d(\ln \bar{r}\bar{\mu})/d\bar{s} \quad (11)$$

This equation can be integrated using the compressible flow correction to the Prandtl skin-friction law, which results in

$$N_{R\theta} = \frac{0\,037\bar{N}_R^{0\,8}}{\bar{\mu}\bar{r}\varphi^{0\,4}}\left[\int_0^{\bar{s}} \bar{\rho}\bar{u}(\bar{\mu}\bar{r})^{5/4}d\bar{s}\right]^{0\,8} \quad (12)$$

Combining Eqs (10) and (12), the nondimensional mass flow parameter becomes

$$\frac{m_0}{r^*\mu_s \bar{N}_R^{0\,8}} = \frac{0\,232}{\varphi^{0\,4}}\left[\frac{\delta}{\theta} - \frac{\delta^*}{\theta}\right]\left[\int_0^{\bar{s}} \bar{\rho}\bar{u}(\bar{\mu}\bar{r})^{5/4}d\bar{s}\right]^{0\,8} \quad (13)$$

and, therefore,

$$\frac{m_c}{m_0} = \frac{\bar{N}_1\varphi_{s_c}^{0\,4}}{0\,232}\left[\frac{\delta}{\theta} - \frac{\delta^*}{\theta}\right]^{-1}\left[\int_0^{\bar{s}} \bar{\rho}\bar{u}(\bar{\mu}\bar{r})^{5/4}d\bar{s}\right]^{-0\,8} \quad (14)$$

The ratios of boundary-layer thickness and displacement thickness to momentum thickness are tabulated, as a function of the external Mach number and wall-to-freestream temperature ratio, by Persh and Lee [28] Therefore, if the nozzle geometry, wall temperature, and stagnation conditions of the fluid are known, the ratio of coolant mass to zero injection mass flow can be determined as a function of the mass-transfer similarity parameter $\bar{N}_1$ from Eq (14) For a given coolant fluid and specified coolant temperature, the effective adiabatic wall temperature can be determined from Eq (9) The present experimental data, however, correspond to the heat-transfer distribution for a given wall temperature distribution rather than the wall temperature resulting from zero heat transfer As a result, the adiabatic wall temperature obtained from Eq (9) must be used to form a reduced heat-transfer coefficient or Nusselt number This can be done by using the observed variation of heat-transfer coefficient with mass transfer in a laminar boundary layer ¶ If this approximation is used, the local Nusselt number with mass transfer can be computed from the zero injection value thereof as follows:

$$Nu/\bar{N}_R^{0\,8} = (Nu/\bar{N}_R^{0\,8})_0[(h_{aw} - h_w)/(h - h_w)] \quad (15)$$

This calculation has been performed for the present geometry and test conditions, and the curves resulting therefrom are included in Figs 2a–2h with the experimental data; the solid lines denote the results of the analysis using nitrogen as the coolant fluid, whereas the dashed lines correspond to the helium coolant The zero injection heat-transfer theory used in Eq (15) is that obtained from the FPRE method It is seen that the analysis is in good agreement with the experimental data when applied a sufficient distance downstream of the injection location, but is relatively poor in the vicinity of the mass-transfer region This can be partially attributed to the fact that the predicted curves depend directly upon the theoretical zero injection heat-transfer rate, which has not been verified experimentally in this region

The present analysis of the downstream influence of mass transfer has also been applied to the experimental conditions of Ref 10, which presents recovery temperature data in an incompressible turbulent boundary layer with zero pressure gradient The data correspond to external flow velocities between 20 and 100 fps, to atmospheric pressure, and to temperature differences of approximately 90°R Wall temperature measurements were obtained for a steady-state condition, the surface thermocouples thus indicating the local adiabatic wall temperature of the flow The data were obtained over a region extending from the edge of the porous surface to roughly 50 injection lengths downstream of the mass transfer These data are reproduced in Fig 4, where the adiabatic wall temperature is presented as a function of the nondimensional mass-transfer parameter (B) derived in Ref 10 The parameter B can be related to the present mass-transfer parameter $\bar{N}_1$ by the following:

$$B = Re_x^{0\,8}/(\bar{N}_1\bar{N}_R^{0\,8}) \quad (16)$$

If Eq (10) is modified to apply to a two-dimensional, incompressible flow, the mass flow ratio reduces to

$$m/m_0 = 3\bar{N}_1\bar{N}_R^{0\,8}/Re_x^{0\,8} = 3\,0/B \quad (17)$$

Combining Eqs (9) and (17) for homogeneous coolant injection and for a constant specific heat yields

$$(T_e - T)/(T_e - T_{aw}) = 1 + m_0/m = 1 + B/3 \quad (18)$$

This result is presented in Fig 4, along with the experimental data and integral method analysis of Ref 10 It is seen that the present method gives quite good agreement with the data, except in close proximity to the porous region where

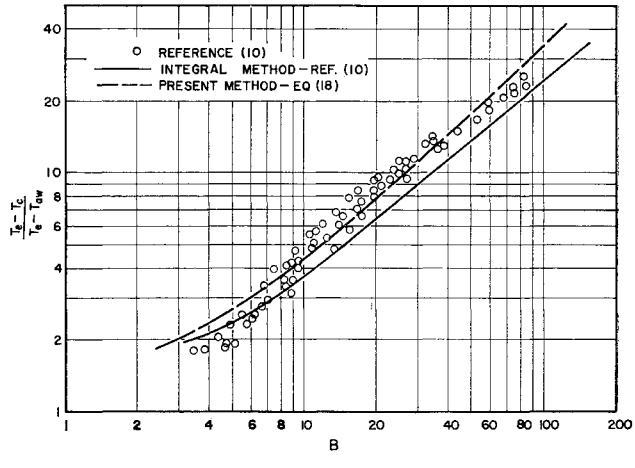

Fig 4 Comparison of theory and experiment for incompressible turbulent layer

¶ In Ref 14, both the adiabatic wall enthalpy and the local heat-transfer rate downstream of a mass transfer region were measured experimentally for the same rates of injection These data were used to compute heat-transfer coefficients based on the local measured values of the adiabatic wall enthalpy For each surface location, it was found that the resulting heat transfer coefficient was independent of the mass-transfer rate within the experimental accuracy of the data

the experimental data indicate a lower surface temperature than the analysis predicts This is to be expected, however, since the basic hypothesis of the present method considers the coolant and external flows to be completely mixed at the junction of the permeable and impermeable surface In reality, the effective temperature of the fluid near the wall is probably lower than in the remaining portion of the layer, in the vicinity of the injection region However, the agreement between the present analysis and the experimental data improves considerably in the downstream direction

Concluding Remarks

An experimental investigation of the downstream influence of mass transfer on an axisymmetric nozzle in turbulent flow has been carried out The coolant gases (helium and nitrogen) were injected at various rates through a porous region upstream of the throat of the nozzle The experimental heat transfer to the nozzle surface is presented as a function of the mass transfer for various stations along the impermeable region of the nozzle

An approximate method for predicting the influence of the mass injection on the adiabatic wall temperature and heat transfer downstream of a transpiration-cooled region was developed This method agrees reasonably well with the experimental data for stations sufficiently downstream of the porous region The applicability of the method is further demonstrated by comparison with some available incompressible data

In order to determine the effectiveness of mass-transfer cooling in a practical application, a numerical example was considered for a typical nozzle contour A contraction-area ratio of 8 to 1 was assumed with a convergent semivertex angle of 45° The coolant mass required to restrict the wall temperature at the throat to 2000°R was computed with helium as a coolant The coolant is assumed to be injected sufficiently upstream of the throat to cool the entire subsonic flow surface as in the present experimental configuration For a chamber stagnation enthalpy of 5000 Btu/lb and a chamber pressure of 100 atm, the heat transfer to the throat with no cooling is approximately 11,000 Btu/ft²-sec In order to cool the throat to a temperature of 2000°R, the amount of helium required corresponds to 18% of the total mass flowing through the nozzle As the chamber pressure increases, for the same chamber enthalpy, the ratio of required coolant mass to total mass flowing through the nozzle decreases Since lower heat-transfer rates are associated with lower chamber pressures, nozzles operating under these conditions can be effectively cooled by other methods For high-enthalpy, high-pressure applications, however, transpiration cooling appears to be an extremely useful technique

References

[1] Eckert, E R G and Livingood, J N B, "Comparison of the effectiveness of convection, transpiration and film cooling methods with air as coolant," NACA TR 1182 (1954)

[2] Rubesin, M W, "An analytical estimation of the effect of transpiration cooling on the heat transfer and skin friction characteristics of a compressible turbulent boundary layer," NACA TN 3341 (December 1954)

[3] Rubesin, M W and Pappas, C C, "An analysis of the turbulent boundary layer characteristics on a flat plate with distributed light gas injection," NACA TN 4149 (February 1958)

[4] Rubesin, M W, "The influence of surface injection on heat transfer and skin friction associated with the high-speed turbulent boundary layer," NACA RM A55L13 (February 1956)

[5] Black, T J and Sarnecki, A J, "The turbulent boundary layer with suction or injection," Aeronaut Res Council, ARC 20,501, F M 2745 (October 1958)

[6] Mickley, H S, Ross, R C, Squyers, A C, and Stewart, W E, "Heat, mass and momentum transfer for flow over a flat plate with blowing or suction," NACA TN 3208 (July 1954)

[7] Leadon, B M and Scott, C J, "Transpiration cooling experiments in a turbulent boundary layer at $M = 3.0$," J Aeronaut Sci **23**, 798–799 (1956)

[8] Pappas, C C and Okuno, A F, "Measurements of skin friction of the compressible turbulent boundary layer on a cone with foreign gas injection," J Aerospace Sci **27**, 321–333 (1960)

[9] Bartle, E R and Leadon, B M, "The compressible turbulent boundary layer on a flat plate with transpiration cooling," Convair Sci Res Lab., Res Rept 11 (May 1961)

[10] Nishiwaki, N, Hirata, M, and Tsuchida, A, 'Heat transfer on a surface covered by cold air film," *International Developments in Heat Transfer* (American Society of Mechanical Engineers, New York, September 1961), pp 675–681

[11] Bernicker, R P, "An experiment with a transpiration cooled nozzle,' Mass Inst Tech, Naval Supersonic Lab, TR 447, Air Force Office Sci Res TN 60 1484 (July 1960)

[12] Cresci, R J, MacKenzie, D A, and Libby, P A, "An investigation of laminar, transitional and turbulent heat transfer on blunt nosed bodies in hypersonic flow," J Aerospace Sci **27**, 401–414 (1960)

[13] Libby, P A and Cresci, R J, "Evaluation of several hypersonic turbulent heat transfer analysis by comparison with experimental data," Polytechnic Inst Brooklyn, PIBAI Rept 387, Wright Air Dev Center TN 57-72 (July 1957)

[14] Libby, P A and Cresci, R J, "Experimental investigation of the downstream influence of stagnation point mass transfer," J Aerospace Sci **28**, 51–64 (1961)

[15] Penner, S S, *Chemistry Problems in Jet Propulsion* (Pergamon Press, New York, 1957), Chap XIII

[16] Hirschfelder, J O, Curtiss, C R, and Bird, R B, *Molecular Theory of Gases and Liquids* (John Wiley and Sons, Inc, New York, 1954)

[17] Lane, F, "Solution of transient heat equation for an axisymmetrically heated shell of revolution," Gruen Applied Sci Labs, Inc (January 1958)

[18] Cresci, R J and Libby, P A, 'The downstream influence of mass transfer at the nose of a slender cone," J Aerospace Sci **29**, 815–826 (1962)

[19] Bartz, D R, "A simple equation for rapid estimation of rocket nozzle convective heat transfer coefficients," Jet Propulsion **27**, 49–51 (1957)

[20] Eckert, E R G, "Survey on heat transfer at high speeds," Wright Air Dev Center TR 54-70 (1954)

[21] Massier, P F, Gier, H. L, Witte, A B, and Harper, E Y, "Heat transfer and fluid mechanics," Jet Propulsion Lab, Calif Inst Tech, Res Summary 36-11 (November 1, 1961)

[22] Welsh, W E and Witte, A B, "A comparison of analytical and experimental local heat fluxes in liquid propellant rocket thrust chambers" Jet Propulsion Lab TR 32-43 (February 1, 1961)

[23] Zakkay, V and Callahan, C J, "Laminar, transitional and turbulent heat transfer to a cone-cylinder flare body at Mach 8.0," J Aerospace Sci **29**, 1403–1413, 1420 (1962)

[24] Aiello, G F, "An investigation of a three-dimensional turbulent boundary layer in hypersonic flow," Polytechnic Inst Brooklyn, PIBAL Rept 773 (December 1962)

[25] Howe, J T, "Some finite difference solutions of the laminar compressible boundary layer showing the effects of upstream transpiration cooling," NASA Memo 2-26-59A (1959)

[26] Pallone, A J, "Non-similar solutions of the compressible laminar boundary layer equations with applications to the upstream transpiration cooling problem," J Aerospace Sci **28**, 449–456 (1961)

[27] Cresci, R J, "Theoretical analysis of the downstream influence of mass transfer in a stagnation region," Intern J Heat Mass Transfer **5**, 837–857 (1962)

[28] Persh, J and Lee, R, "Tabulation of compressible turbulent boundary layer parameters," U S Naval Ordnance Test Station NAVORD Rept 4282 (May 1956)

[29] Librizzi, J and Cresci, R J, "Transpiration cooling of a turbulent boundary layer in an axisymmetric nozzle," Polytechnic Institute of Brooklyn, PIBAL Rept 772 (February 1963)